Available online at www.sciencedirect.com
SCIENCE DIRECT®
Remote Sensing of Environment 98 (2005) 494 – 510
Remote Sensing of Environment
www.elsevier.com/locate/rse

Stormwater runoff plumes observed by SeaWiFS radiometer in the Southern California Bight

Nikolay P. Nezlin [a,*], Paul M. DiGiacomo [b], Eric D. Stein [a], Drew Ackerman [a]

[a] Southern California Coastal Water Research Project, Westminster, CA 92683, USA
[b] Jet Propulsion Laboratory, California Institute of Technology, Pasadena, CA 91109, USA

Received 4 May 2005; received in revised form 19 August 2005; accepted 25 August 2005

Abstract

Understanding the factors that influence the incidence and dispersal patterns of freshwater runoff plumes in southern California is important for management of coastal water quality. Significant river discharge is associated with episodic winter rainstorms, leading to turbid pollutant and pathogen-laden stormwater plumes that are clearly visible nearshore in the Southern California Bight. We analyzed 1.1-km spatial resolution sea-spectral reflectance data acquired in 1997–2003 by the Sea-viewing Wide Field-of-view Sensor (SeaWiFS), focusing on four regions with distinctive adjacent watershed properties: Ventura, Santa Monica Bay, San Pedro Shelf, and Orange County/San Diego. The area of each plume was detected by the backscattering characteristics of surface waters, i.e., normalized water-leaving radiation of green–yellow wavelength 555 nm (nLw555). Plume area size was correlated with the rainstorm magnitude, which was estimated from atmospheric precipitation averaged over the total area of the watersheds connected to the seashore. The time lag between rainstorm and maximum plume was one day in San Pedro Shelf and two days in other three regions. Assessing maximum correlation between precipitated rainwater and the plume size, we estimated the optimal nLw555 values best characterizing the plume boundaries in each of the four study regions. Another quantitative characteristic derived from maximum correlation between rainwater and plume size was the "coefficient of persistence", related to the speed of freshwater discharge and the time of plume water dissipation; it was also different in different watersheds. The primary factors regulating the relationship between rainstorm and plume were watershed land-use characteristics, size, and elevation.

Keywords: Ocean color; Sea-spectral reflectance; Freshwater discharge; Plumes; Precipitation; Southern California Bight; 32°00′–34°30′N; 120°00′–117°00′W

1. Introduction

Water quality in the Southern California Bight (SCB; Fig. 1) is impacted by seasonally variable river runoff. The runoff is a primary source of contaminants that can negatively impact human and ecosystem health and productivity (Ackerman & Weisberg, 2003; Bay et al., 2003; Noble et al., 2003; Reeves et al., 2004; Schiff & Bay, 2003). Winter rainstorm events lead to episodic peaks in runoff, often resulting in high near-shore bacterial counts that can force closures of recreational beaches due to associated human health risks (Cabelli et al., 1982; Haile et al., 1999). Strong rainstorms are especially hazardous, because the concentration of bacteria in storm water increases with increasing rainstorm intensity (Reeves et al., 2004). Intensive storm water discharge after rainstorms produce plumes that are easily distinguished from ambient marine waters by their high concentration of suspended matter that changes the color of the ocean surface (Mertes et al., 1998; Mertes & Warrick, 2001; Sathyendranath, 2000). The movement and persistence of plumes may be influenced by a variety of factors, such as wind and ocean circulation, as well as the volume, timing and intensity of storm water discharge. Knowledge of the factors influencing and regulating plume dynamics is important for coastal managers, who are responsible for short-term management and long-term policy decisions to protect water quality and human health for the millions of residents who annually use southern California beaches and coastal waters.

Storm water plumes are typically studied using data collected from buoys and research vessels. However, such traditional oceanographic methods cannot resolve detailed

* Corresponding author. Fax: +1 714 894 9699.
E-mail address: nikolayn@sccwrp.org (N.P. Nezlin).

0034-4257/$ - see front matter © 2005 Elsevier Inc. All rights reserved.
doi:10.1016/j.rse.2005.08.008

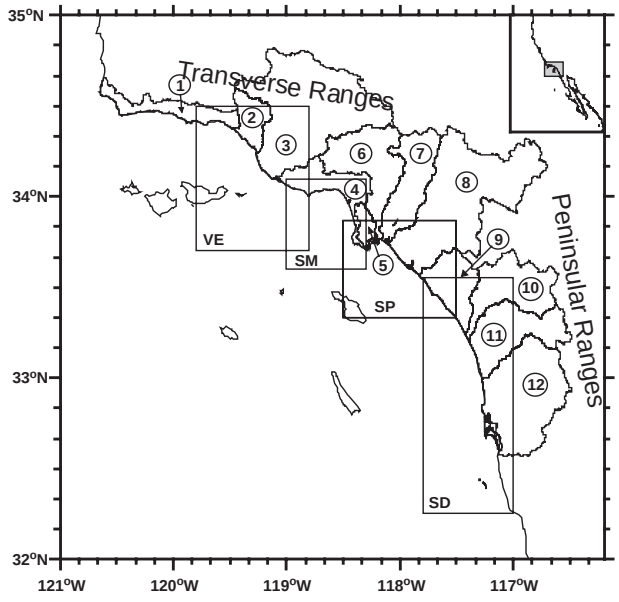

Fig. 1. The scheme of the study area of the Southern California Bight. The rectangles indicate the areas of the regions where the plumes were analyzed: VE—Ventura; SM—Santa Monica Bay; SP—San Pedro Shelf; SD—Orange County/San Diego. The numerals in circles indicate the coastal watersheds where the rainstorm magnitude was estimated (Table 1).

spatio-temporal patterns of stormwater plume dynamics due to a characteristically limited number of stations (and/or samples) resulting from logistics, cost, weather, or other constraints. This problem can be partly solved by utilizing existing satellite observations of visible spectral radiance (~ocean color), regularly (nominally daily) collected by NASA imaging spectroradiometers in low Earth orbit (e.g., Esaias et al., 1998; McClain et al., 2004). Cloud cover leading to missing data is a common occurrence and challenge when using ocean color imagery, but it is somewhat mitigated in southern California by the high pressure systems that often follow winter storms and typically serve to clear the skies in this region, as well as by the daily acquisition of ocean color data. Level 2 (1.1-km spatial resolution) data and associated imagery from the Sea-viewing Wide Field-of-view Sensor (SeaWiFS) collected since autumn 1997 provide an extensive data set for statistical analysis of plume dynamics, and investigation of potential controlling factors, in different sub-regions of the southern California coastal zone.

In this study, we analyze discharge-plume dynamics in four regions of the SCB (Fig. 1). In a previous study based on SeaWiFS observations, Nezlin and DiGiacomo (2005) analyzed the statistical relationship between the amount of precipitated stormwater and the dynamic characteristics of plumes over the San Pedro Shelf, adjacent to a highly urbanized coastal watershed. They estimated that normalized water-leaving radiation at 555 nm (~green–yellow band) of a level >1.3 mW cm^{-2} μm^{-1} sr^{-1} appeared to be the best fit for distinguishing the runoff plume from ambient waters. The persistence of plumes was estimated by fitting the coefficients of the model of plume water dissipation (see Eq. (1) in Methods) to achieve maximum correlation between the plume area and rainstorm. It remained unclear, however, to what extent the observed relationships were applicable to other areas of SCB. Comparing the quantitative relations between rainstorm and plume size off different regions of the southern California coast, we focus on the differences between the catchment areas (watersheds) where stormwater is precipitated, infiltrated and discharged to the coastal ocean.

Our goals are:

- To quantify areas of runoff plumes within the SCB using SeaWiFS observations from October 1997 to June 2003, specifically identifying nLw555 values that serve as the optimal plume boundary indicator in different regions;
- To explore the correlation between plume area and the amount of stormwater discharged from coastal watersheds in different sub-regions of the SCB, with a focus on the time lag between rainstorms, extent of plume and persistence of the plume;
- To describe typical sizes and patterns of stormwater plumes in different regions of the SCB;
- To relate the correlations between rainstorms and plumes with the physiographic and land-use characteristics of watersheds.

2. Coastal watersheds in Southern California

In this study, we analyze statistical relationships between freshwater discharge and plume size in four rectangular ocean regions in the near-shore zone of the SCB (Fig. 1). Satellite-sensed visible spectral radiance (ocean color) data were obtained, processed, and analyzed within the part of each rectangle (VE, SM, SP, and SD at Fig. 1) that contained ocean data. Each ocean region was associated with the group of coastal watersheds (1–12 at Fig. 1; see also Table 1), within

Table 1
Coastal watersheds of the Southern California Bight

#	Watershed	Area (km^2)	Number of analyzed rain gauge stations
1	Santa Barbara Creek	971	2
2	Ventura River	696	2
3	Santa Clara River	5164	12
	Ventura region (total)	6831	16
	Malibu Creek	286	
	Ballona Creek	338	
4	Santa Monica Bay region (total)	1170	7
5	Dominguez Channel	300	2
6	Los Angeles River	2161	13
7	San Gabriel River	1758	10
8	Santa Ana River	5101	13
	San Pedro Shelf region (total)	9320	38
9	San Juan Creek	1284	2
10	Santa Margarita River	1915	4
11	San Luis Rey River/ Escondido Creek	2002	3
12	San Diego Creek	3561	16
	Orange County/San Diego region (total)	8762	25

which freshwater runoff originated, primarily from the water precipitated during rainstorms.

Rainfall and runoff patterns throughout the southern California region are governed by a complex combination of atmospheric circulation and topographic effects. Low-pressure winter storms typically move southward from the North Pacific along the western edge of North America. As these storm systems approach southern California, they are moderated by the Pacific high-pressure system and a thermal low to the east, which deflects many storms (Bailey, 1966). As a result, the average annual rainfall in southern California is only 30 cm (12 in.), less than a third of the northern part of the California State (Beuhler, 2003). During winter, the center of high pressure moves to a southwest position, allowing brief, intense Pacific storm fronts to penetrate the area (Lu et al., 2003). Rainfall patterns are further moderated by a temperature inversion created by the ring of mountain ranges that define southern California. The east–west Transverse Ranges and the north–south Peninsular Ranges create a "coastal basin" where cool, dense air is trapped, often deflecting marine winds over the area, resulting in much weaker wind patterns than over the open ocean and lower rainfall than areas to the east (Dorman & Winant, 1995).

Runoff from the southern California coastal watersheds is typically manifested as brief, intense episodes. Coastal watersheds are short and steep, dropping from almost 3000 m in elevation to sea level, often in less than 200-km distance. The dynamic nature of runoff is exacerbated by land-use practices that are typical of most coastal areas. A population of approximately 20 million people is concentrated in a relatively narrow band of land along the coastal plain (Schiff et al., 2000b). The impervious surfaces associated with these developed areas increase the magnitude and intensity of storm water runoff, and associated loadings of contaminants, nutrients, and other pollutants, to the coastal ocean.

Although runoff from all southern California coastal watersheds is influenced by the regional factors described above, there are some key differences between the four sub-regions. Differences that may affect runoff patterns are related to the trend of decreasing precipitation from the northern to southern watersheds (Beuhler, 2003; Nezlin & Stein, 2005) and the increasing role of the peninsular ranges in attenuating runoff from the southern watersheds.

The northern part of the SCB is associated with three watersheds, Santa Barbara Creek, Ventura River, and Santa Clara River. The largest is the 5164 km^2 Santa Clara River watershed. The Ventura River and Santa Barbara Creek watersheds are much smaller (696 and 971 km^2, respectively; Table 1). These watersheds are the least developed of the region (in terms of the percent of watershed area) and are dominated by forest, chaparral and coastal sage scrub. In addition, there is little hydrologic control in terms of major dams or flood control channels. The lack of hydrologic control, combined with the typically higher rainfall than more southern watersheds, translates to high volumes of sediment-laden discharge following episodic rain events. Because the outlets of the Ventura and Santa Clara rivers are located close to each other (within 5 km), the discharges of these two rivers commingle and cannot be distinguished at 1.1-km resolution satellite images.

The Malibu and Ballona Creek watersheds, as well as several small watersheds draining the Santa Monica Mountains, discharge to the Santa Monica Bay. This area lies within the northern portion of the Transverse Ranges, which are characterized by very short and steep watersheds. Malibu Creek watershed is approximately 15% developed, with those areas concentrated in two portions of the watershed, which have been shown to produce high nutrient (Schiff & Bay, 2003) and bacteria loads. With the exception of several tributaries, most of the creeks in the Malibu watershed are not channelized. In contrast, the Ballona Creek watershed is approximately 85% developed and the streams consist entirely of concrete channels or underground storm drains. The remaining short, steep watersheds draining the Santa Monica Mountains are mainly undeveloped.

The San Pedro Shelf receives discharge from four watersheds totaling 9320 km^2 of drainage area: Dominguez Channel, Los Angeles, San Gabriel, and Santa Ana rivers (Table 1). These four watersheds constitute the most populated areas of southern California. Consequently, the streams are highly modified with numerous dams, diversions, and channels that tightly control runoff and have attenuated peak flows from historic levels (Booth, 1990; Dunne & Leopold, 1978). The greater Los Angeles basin is a series of overlapping floodplains ringed in mountains. In addition, this area was under water as recently as the Pleistocene period, less than 2 million years ago. The combination of marine and fluvial processes has resulted in a mix of marine and continental sedimentary materials that form deep alluvial aquifers along most of the coastal plain. Consequently, much of the surface runoff is diverted for ground water recharge prior to reaching the coast.

The southern-most Orange County/San Diego Region is associated with 12 major and several minor watersheds. The larger watersheds include San Diego Creek, San Juan Creek, Santa Margarita River, San Luis Rey River, Escondido Creek, and San Diego River watersheds. The total area of these coastal watersheds is 8762 km^2. This portion of the coast is distinct in that the watersheds generally drain to the west (as opposed to the south). This orientation contributes to drier and more temperate conditions than other portions of southern California. In addition, the southern watersheds overlap both the Peninsular and Transverse Ranges resulting in bimodal longitudinal profiles. In the upper portions of the watersheds, water drains from the steep mountains of the transverse ranges to inland alluvial valleys. Water then flows down and across the lower peninsular ranges onto broad coastal terraces before discharging to the ocean. The inland valleys are often separated from the coastal terraces by steep, narrow gorges. This watershed physiography acts to attenuate water and sediment flow to the coast.

3. Methods

Remotely sensed normalized water-leaving radiation at 555-nm wavelength (nLw555; green–yellow band) was used to

discriminate and contour freshwater plumes. Otero and Siegel (2004) showed that nLw555 is better correlated with the concentration of suspended sediments in near-surface waters than other wavelengths and, hence, is a good proxy for the water discharged from river mouths after rainstorms. The nLw555 values were derived from SeaWiFS (McClain et al., 2004) data collected between October 6 (Julian Day 279) 1997 and June 26 (Julian Day 177) 2003. High-resolution (1.1-km) SeaWiFS Level 1A data were obtained from National Aeronautics and Space Administration Goddard Space Flight Center Distributed Active Archive Center (NASA GSFC DAAC) (Acker et al., 2002) and processed using SeaDAS software (Version 4.3). To calculate nLw555 normalized water-leaving radiances (Level 2 data), near-coincident NCEP meteorological and EPTOMS and TOVS ozone data files were obtained from GSFC DAAC and applied to corresponding SeaWiFS Level 1A data. We used the standard SeaDAS algorithm with the "land", "cloud", and "stray light" flags among others applied as masks.

In each of the four study regions (Fig. 1), nLw555 pixel values from each SeaWiFS scene were interpolated on a regular grid of spatial resolution $0.01° \times 0.01°$ (about 1 km). "Missing data" (MD) values were applied to the grid nodes located >2 km from the nearest "non-missing" pixel. The resulting images were visually analyzed to select the grids where clouds did not cover the coastal zone and the pattern of the freshwater plume was visible. Nevertheless, some of the selected images were partly covered by clouds. A stripe between the coast and the

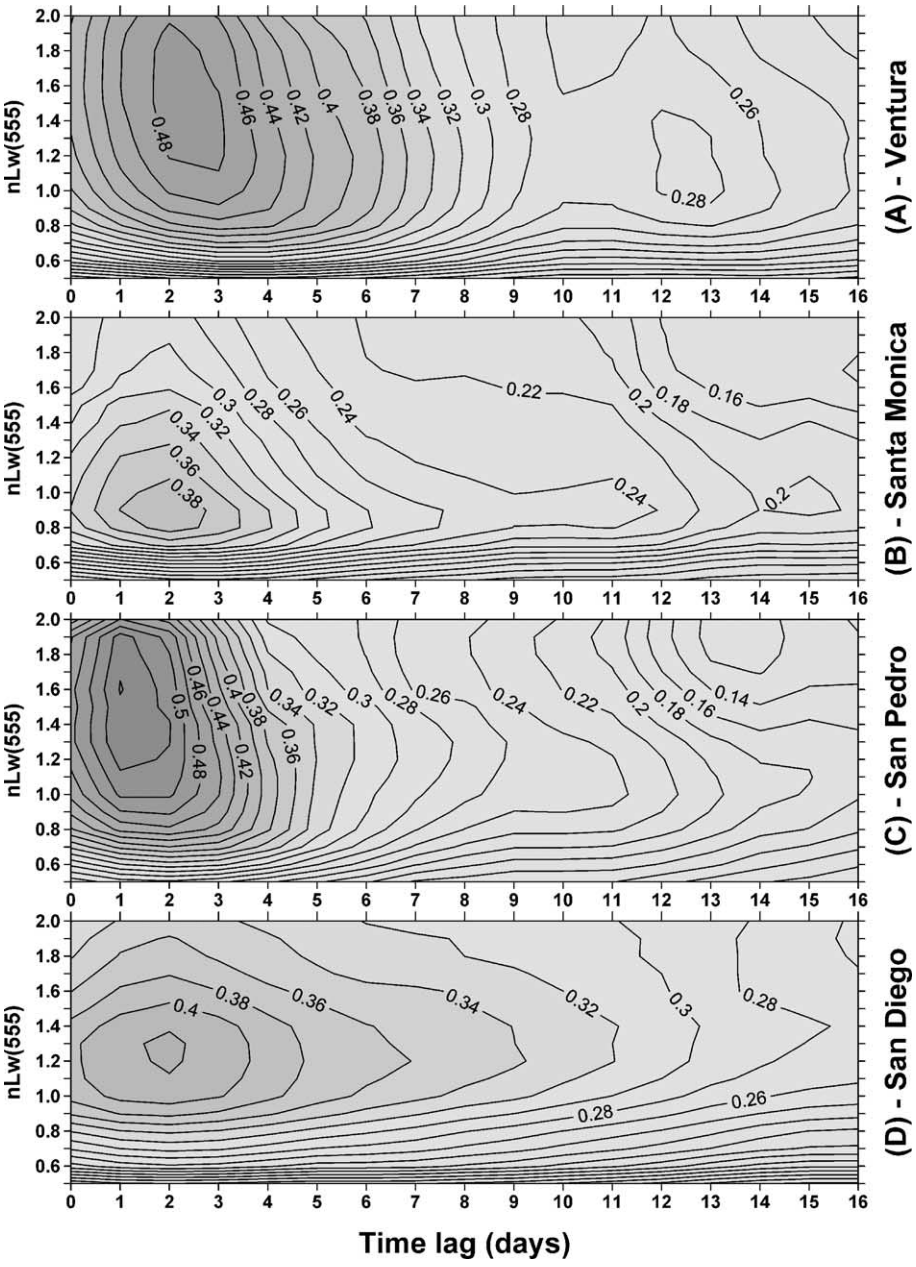

Fig. 2. 2D-diagrams of the correlations between the freshwater plume areas (bounded by different nLw555 levels) and the rainstorm magnitudes in the adjacent watersheds at different time lags. Ventura area (A); Santa Monica Bay (B); San Pedro Shelf (C); Orange County/San Diego area (D).

ocean also often contained MD because of "stray light" mask effect. To quantitatively estimate the plume area at these images, we filled the ocean zones containing MD (i.e., covered by clouds) with interpolated nLw555 values. The grid nodes containing MD and located near the nodes with "non-missing" data were replaced with the interpolated nLw555 values obtained by averaging the surrounding grid nodes using a 3×3 Gaussian filter. Each step of this operation added "non-missing" data at the edge between the "non-missing" and MD (covered by clouds) areas. This operation was repeated until all grid nodes in the ocean zone were filled with "non-missing" data. Land masks were applied to the grids to remove (i.e., replace by MD) the data unintentionally interpolated over the land. This iterative process was visually controlled to avoid a substantial distortion of plume contour; if this happened, the image was removed from the analysis.

The total number of analyzed SeaWiFS scenes (October 1997–June 2003) was 493 in Ventura region, 268 in Santa Monica Bay, 628 in San Pedro Shelf region, and 320 in Orange County/San Diego region. During other days no SeaWiFS observations were obtained due to cloudy weather/no available data over the SCB. In each scene, the plume area was estimated on the basis of the area covered by waters with high nLw555 index. The level of nLw555 indicator value to distinguish between the plume and the ambient waters was initially unknown; the goal of the study was to select the nLw555

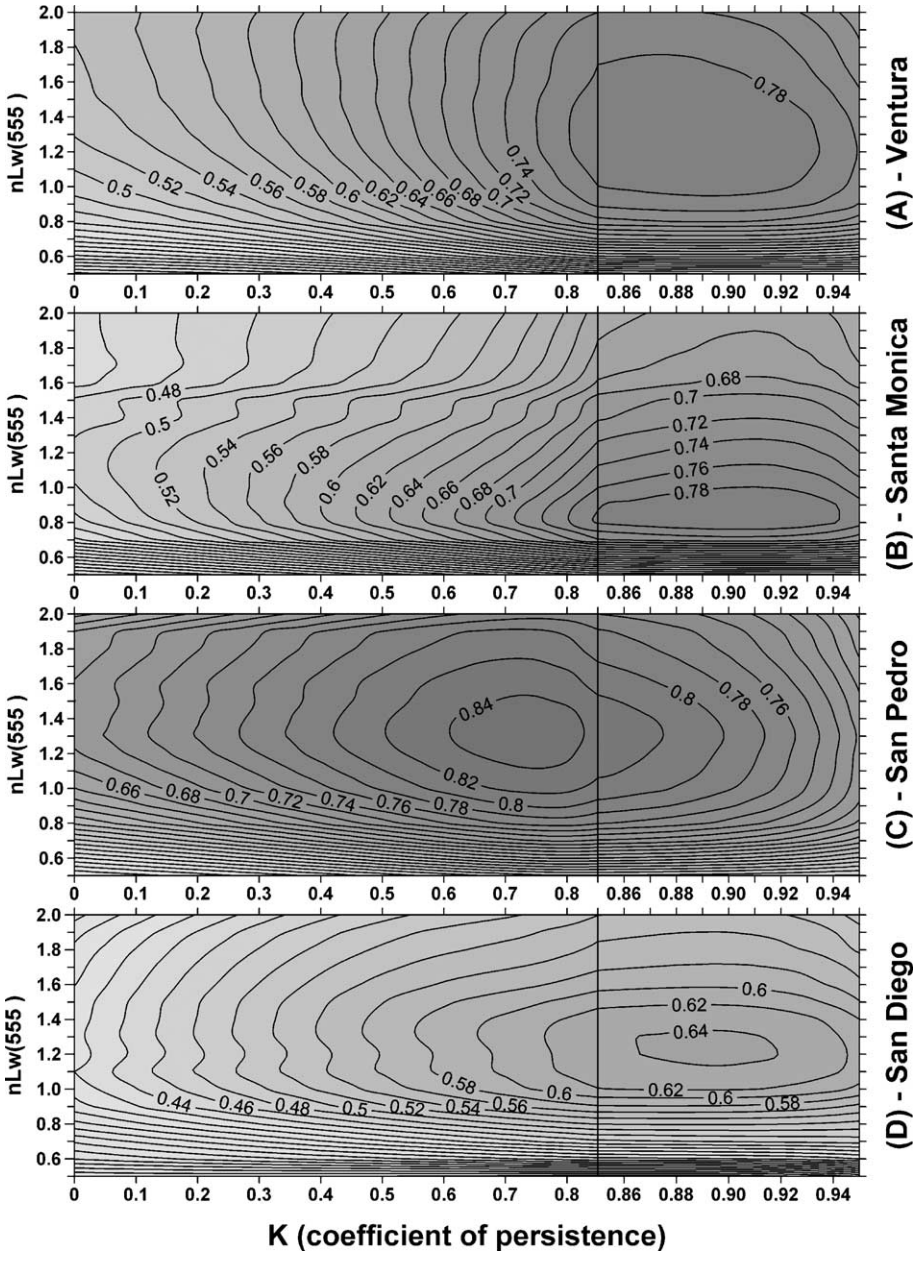

Fig. 3. 2D-diagrams of the correlations between the freshwater plume areas bounded by different nLw555 levels (*Y*-axis) and the precipitated water accumulated over the adjacent watersheds and estimated with different coefficients of persistence (k, *X*-axis). Ventura area (A); Santa Monica Bay (B); San Pedro Shelf (C); Orange County/San Diego area (D). Note the change of the scale of *X*-axis at 0.85.

Table 2
Statistical characteristics of the maximum correlations between freshwater plume areas and accumulated rainwater in four regions of southern California

Region	nLw555 (mW cm^{-2} μm^{-1} sr^{-1})	k (coefficient of plume persistence, see Eq. (1))	Maximum correlation (R)
1. Ventura	1.3	0.89	$R=0.7995$
2. Santa Monica Bay	0.8	0.90	$R=0.7981$
3. San Pedro Shelf	1.3	0.75	$R=0.8516$
4. Orange County/San Diego	1.2	0.90	$R=0.6432$

indicator which best characterizes the plume boundary in different regions. For this, we tested the "plume boundary" threshold levels within the range from 0.5 to 2.0 mW cm^{-2} μm^{-1} sr^{-1}; the nLw555 level bounding the plume area that best correlated with stormwater discharge was selected as a plume indicator.

Rainstorm magnitude was estimated from the atmospheric precipitation averaged over four combined watersheds related to the four study regions (Fig. 1; Table 1). Daily rain gauge data from 98 meteorological stations located in these watersheds were downloaded from the National Oceanic and Atmospheric Administration National Data Center Climate Data Online (NNDC/CDO) Internet site. Each observation represents the precipitation during a 24-h period preceding the observation time. The precise time of observation varied between the stations during different periods; therefore, we attributed each observation to an entire day and did not analyze the variability at a sub-diurnal time-scale. Not all stations had continuous data for the entire 6-year period of analysis; so, the average precipitation for each day from October 1997 till June 2003 was estimated from a variable number of stations (see details in Nezlin & Stein, 2005).

The analysis of correlation between the rainstorm and the plume area is based on the model of linear "signal/response" dependence between these two parameters. To obtain a quantitative statistical evaluation of the response of the plume size as estimated by an area occupied by water with nLw555 exceeding the selected threshold to the rainstorm signal, we calculated the time-lagged linear Pearson correlation coefficients between the plume area and the rainstorm magnitude. Different levels of nLw555 were used to find maximum correlation between plume area and rainstorm; the nLw555 resulting in maximum correlation was considered as best plume edge indicator.

To evaluate the persistence of the rainstorm signal in the plume area we estimated for each (t-th) day the precipitated water volume (V_t) accumulated during the previous period by the day preceding the plume, using the equation:

$$V_t = \sum_{i=1}^{t-1} k^{t-i} \cdot P_i = P_{t-1} + k \cdot P_{t-2} + k^2 \cdot P_{t-3} + k^3 \cdot P_{t-4} + k^4 \cdot P_{t-5} + \ldots, \quad (1)$$

where P_i is the precipitation during the i-th day and k is the coefficient of persistence of the freshwater plume. The meaning of k ($0<k<1$) is that during each day the k-th part of the water accumulated during the preceding period is retained in the plume and the $(1-k)$-th part is dissipated. The values of k within the range 0.05–0.95 were tested to obtain best correlation between V_t and the plume area.

To describe typical plume patterns, we estimated the zones where the plumes occurred after rainstorms of different magnitude. Rainstorms were classified into five gradations: <0.25; 0.25–0.6; 0.6–1; 1–2.5; and >2.5 cm of accumulated precipitated water (see Eq. (1)), using the coefficient k resulting in best correlation between rains and plumes in that region. Similar classification of rainstorms (<0.25; 0.25–0.6; 0.6–2.5; and >2.5 cm) was used by Ackerman and Weisberg (2003) studying stormwater discharge to the Santa Monica Bay; we added one more gradation splitting the gradation 0.6–2.5 cm into two (0.6–1 and 1–2.5 cm). For our classification we used accumulated water rather than the magnitude of each rainstorm. The basis of our approach is to avoid the difficulties of the analysis of situations when two or more rainstorms follow each other (a relatively frequent occurrence). The duration of rainstorms in southern California is short, typically 6–12 h (Schiff et al., 2000a); therefore, we do not expect much difference between

Table 3
Coefficients and the analysis of variance of linear ($Y=A+B*X$) and power ($Y=C*X^D$) regression equations between accumulated rainwater (X) and plume area (Y) in four regions of southern California

Region	1. Ventura	2. Santa Monica Bay	3. San Pedro Shelf	4. Orange County/San Diego
Time lag (days)	2	2	1	2
Linear equation	$Y=-5.63+130.22*X$	$Y=-11.13+89.68*X$	$Y=2.96+94.19*X$	$Y=1.10+52.00*X$
Plume variability explained by linear equation (%)	65.4	64.9	72.0	42.3
F (d.f.)	926.0 (1,490)	489.8 (1,265)	1613.4 (1,626)	232.7 (1,317)
p	0.0000	0.0000	0.0000	0.0000
Power equation	$Y=61.92*X^{1.4035}$	$Y=23.14*X^{1.6486}$	$Y=73.62*X^{1.1559}$	$Y=20.20*X^{1.6807}$
Plume variability explained by power equation (%)	75.1	77.9	76.5	58.2
F (d.f.)	739.7 (2,490)	468.4 (2,265)	1021.3 (2,626)	220.9 (2,317)
p	0.0000	0.0000	0.0000	0.0000

Plume boundary nLw555 and accumulated rainwater coefficients of persistence (k) used to estimate the plume/rain relationship are given in Table 2.

the values of accumulated precipitation (Eq. (1)) and total precipitation for a rainstorm that immediately follows a prior rain event. To illustrate the plume patterns in terms of the statistical theory of probability, we estimated for each grid node the percentage of images when this node was attributed to plume. The resulting composites were smoothed by 5-km 2D cosine-filter.

To describe the physiographic differences between watersheds, we used the Digital Elevation Model (DEM) GTOPO30 (USGS, 1996) with a horizontal grid spacing of 30 arc sec (approximately 1 km). The elevations of the DEM grid nodes within the land area of each of four regions (Fig. 1) were tabulated and presented as histograms.

Land cover/land-use data were developed using 30-m resolution LandSat satellite imagery provided by the NOAA Coastal Services Center. These data separate the area into 39 land types based on the standard 22 NOAA Coastal Change Analysis Program (C-CAP) land cover categories. Land-use/land cover classifications are based on year 2000 imagery. We distinguished between six categories of land use:

1) Developed land (both high intensity and low intensity);
2) Cultivated land;
3) Grassland (both managed and naturally occurring);
4) Forests and parks (including deciduous, evergreen, and mixed);
5) Scrubs and shrubs;
6) Wetlands.

In each region we estimated the proportion of the total area occupied by each land-use category.

4. Results

An important issue concerning rainstorm plume dynamics is the time lag between the rainstorm and the resulting plume. Statistical analysis of the time series of precipitation and plume size collected during almost six years of observations (October 1997–June 2003) shows that the time lags between rainstorms and plumes were different in different regions. We explored the correlation between the plume areas estimated from different nLw555 and the daily precipitation averaged over the watersheds of each region (Fig. 2). In three regions (Ventura, Santa Monica Bay, and Orange County/San Diego) maximum correlation was observed at the 2nd day after rainstorm. Over the San Pedro Shelf maximum correlation was observed at the 1st day. The nLw555 values resulting in maximum correlation and, hence, best indicating the plume boundary, were also different in different regions. In Santa Monica Bay, nLw555 was low (0.8–1.0 mW cm^{-2} μm^{-1} sr^{-1}); in Orange County/San Diego region it was 1.2–1.3 mW cm^{-2} μm^{-1} sr^{-1}; in Ventura region and over San Pedro Shelf a wide range of nLw555 coefficients (from 1.2 to 1.9 mW cm^{-2} μm^{-1} sr^{-1}) resulted in high correlation with stormwater. The maximum correlation coefficient was lowest (+0.39) in Santa Monica Bay and higher in San Diego (+0.43) and Ventura (+0.49) regions. Highest correlation was observed over San Pedro Shelf (+0.53).

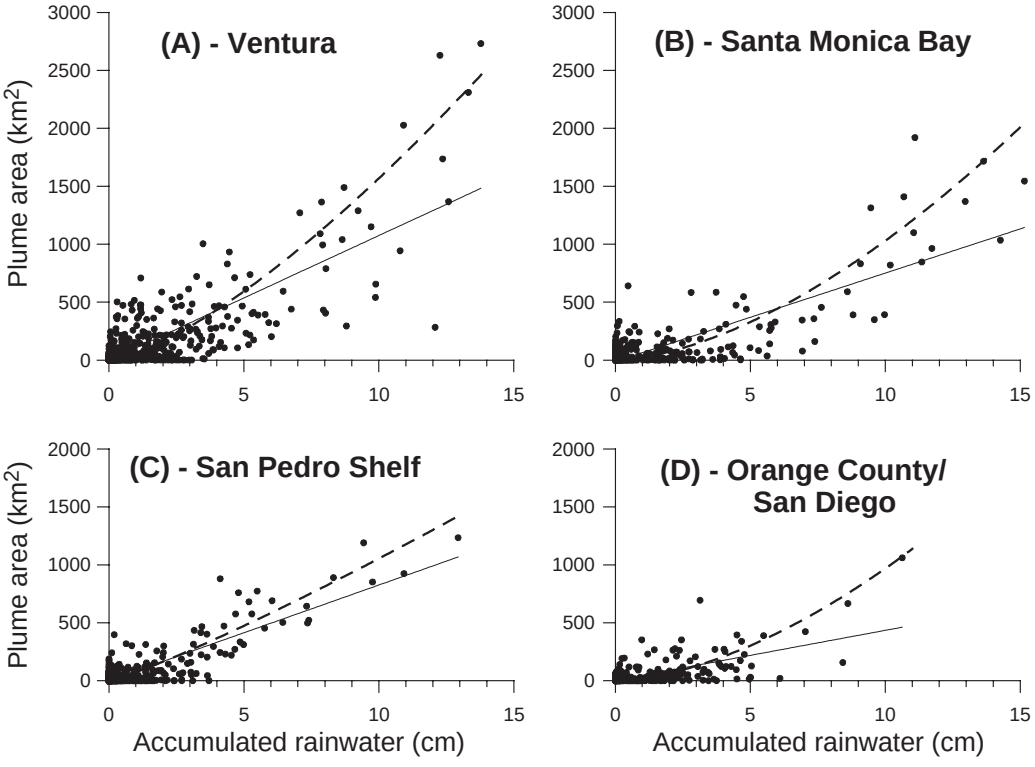

Fig. 4. Linear (solid line) and power (dashed line) relationship between accumulated stormwater and plume area in Ventura region (A); Santa Monica Bay (B); San Pedro Shelf (C); Orange County/San Diego region (D). Plume boundary nLw555 and accumulated stormwater coefficients of persistence (k) used to estimate the plume/rain relationship are given in Table 2, correlation coefficients are given in Table 3.

The persistence of plumes, i.e., the time during which plumes were observed after each rainstorm, was different in different regions. Introducing the "coefficient of plume persistence" (Eq. (1)), we focused on the concept that estimating the correlation between precipitation and plume area, we should take into account not only the stormwater precipitated during the last rainstorm, but the antecedent precipitation as well. To do so, we transformed the precipitation over the watersheds of each of four study regions using Eq. (1) varying the coefficients of persistence (k) within the range of 0.05–0.95. We estimated the correlation coefficients between the transformed precipitation and the plume areas bounded by different nLw555 within the range 0.5–2.0 mW cm^{-2} μm^{-1} sr^{-1}. In all four regions the correlation diagram had one evident maximum (Fig. 3; Table 2). In Ventura, San Pedro, and Orange County/San Diego regions, the nLw555 resulting in a maximum correlation was 1.2–1.3 mW cm^{-2} μm^{-1} sr^{-1}; in Santa Monica Bay it was much lower (0.8 mW cm^{-2} μm^{-1} sr^{-1}). So, we consider the nLw555 indicating plume boundaries to be 0.8 mW cm^{-2} μm^{-1} sr^{-1} in Santa Monica Bay and 1.2–1.3 mW cm^{-2} μm^{-1} sr^{-1} in three other regions. The coefficients of persistence (k) were 0.89–0.90 in Ventura, Santa Monica, and San Pedro regions; over the San Pedro Shelf k was much lower (0.75).

The relationships between accumulated stormwater and plume area estimated on the basis of the optimal time lag, nLw555, and coefficient of persistence k were analyzed in four regions (Table 3; Fig. 4). The intercepts of all four linear equations were insignificantly different from zero. Zero intercept indicates that at zero rainstorm, the size of plume was negligible, i.e., no plume was detected from satellite. At the same time, the slopes of the linear equations were different, indicating that in different regions similar rainstorm magnitude resulted in different plume response. The most prominent response was observed in the Ventura region (1 cm of accumulated stormwater resulted in plume size about 130 km^2). In Santa Monica Bay and San Pedro Shelf 1 cm of rainfall resulted in plume size 90–94 km^2 (keeping in mind that in Santa Monica Bay plumes were detected by nLw555=0.8 vs. 1.3 mW cm^{-2} μm^{-1} sr^{-1} over San Pedro Shelf). In Orange County/San Diego region the relationship was least prominent: about 52 km^2 of plume size per 1 cm of rainfall.

The difference between the slopes of the linear equations became more dramatic after each slope coefficient was normalized to drainage area. For plumes estimated from nLw555=1.3 mW cm^{-2} μm^{-1} sr^{-1}, the ratio between plume size produced by 1 cm of rainfall and drainage area was largest in the Ventura region (0.019); half as large in the San Pedro Shelf (0.010); and lowest in Orange County/San Diego (0.006). The similar ratio for Santa Monica Bay (0.077) could not be compared to other three regions, because plumes there were detected by lower nLw555 (0.8 mW cm^{-2} μm^{-1} sr^{-1}).

Power equations described plume/rain relationship better than the linear relationships in all four regions (Table 3). In the San Pedro Shelf region, the power coefficient (1.156) was close to 1 and the power equation did not differ much from the linear one (Fig. 4C). In the three other regions, the power coefficients (1.40–1.68) were significantly higher than 1 and the power equations more accurately represented the relationship between the accumulated stormwater and the plume area size (Fig. 4A, B, D).

Plume areas were different in each of the four study regions (Fig. 5), varying according to the level of nLw555 indictor used. The optimal nLw555 levels indicating plume boundaries in Santa Monica Bay and in the three other regions were different (0.8 and 1.2–1.3 mW cm^{-2} μm^{-1} sr^{-1}, respectively). To compare the plume areas characteristic of these different regions, we used both aforementioned values (0.8 and 1.3 mW cm^{-2} μm^{-1} sr^{-1}). When the plume was bounded by nLw555=0.8 mW cm^{-2} μm^{-1} sr^{-1}, in Ventura, San Pedro, and Orange County/San Diego regions the plume size distributions were unimodal with maxima at 80–1000 km^2. In these three regions plumes (i.e., the zones of nLw555>0.8 mW cm^{-2} μm^{-1} sr^{-1}) were observed in almost all scenes, during both wet and dry weather. The plumes in the Ventura and San Pedro Shelf regions were largest (most typical size 150–200 km^2); in Orange County/San Diego region the plumes were smaller (100–150 km^2). The plume size

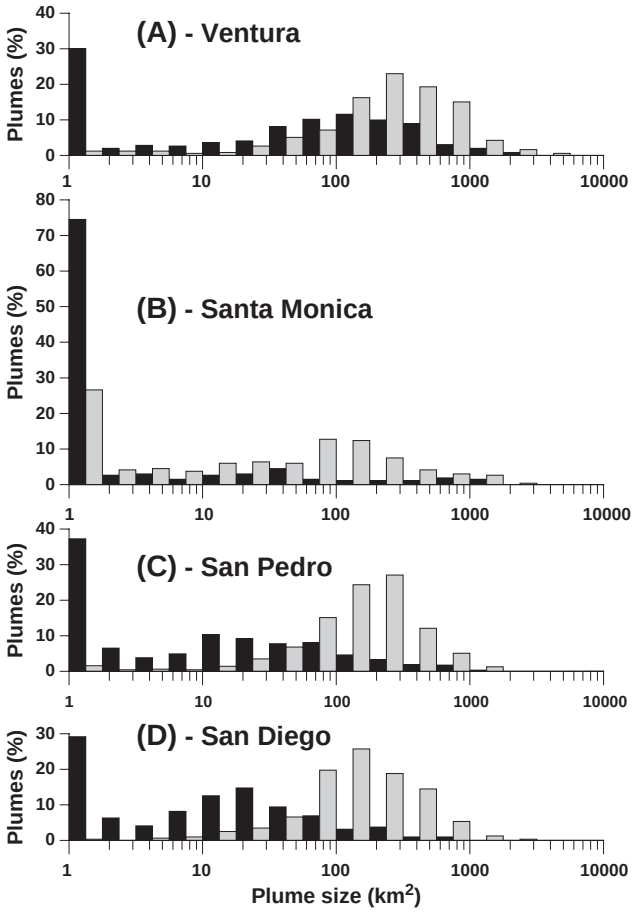

Fig. 5. Size frequency distribution (%) of plumes areas observed in the Ventura (A); Santa Monica Bay (B); San Pedro Shelf (C); and Orange County/San Diego (D) regions during September 1997–June 2003. Black and grey bars indicate plume areas bounded by nLw555 levels 1.3 and 0.8 mW cm^{-2} μm^{-1} sr^{-1}, respectively.

distribution in the Santa Monica Bay was bimodal. The most frequently occurring plume size was <2 km^2 (i.e., no plume); the second maximum of size distribution was at 50–150 km^2.

When the plumes were bounded by nLw555=1.3 mW cm^{-2} μm^{-1} sr^{-1}, the plume size distributions were bimodal in all four regions. Most frequent plume size was <2 km^2; i.e., no plume was observed, at 29–37% of the images in Ventura, Orange County/San Pedro, and San Diego regions and 74% of the images in Santa Monica Bay. The second maximum of size distribution indicated plumes observed after rainstorms. Largest plumes were observed in the Ventura region (100–150 km^2). In Santa Monica Bay, the second maximum was related to plume size 30–60 km^2; however, the number of images with plumes was very small (4.5%). Over the San Pedro Shelf, the range of plume sizes was wide (10–100 km^2). In Orange County/San Diego region typical plume size was 5–40 km^3.

The size of plume area bounded by nLw555>1.3 mW cm^{-2} μm^{-1} sr^{-1} increased with rain magnitude in all four regions. In the Ventura region during dry periods (rain<0.25 cm), plumes occurred only in the mouths of Santa Clara and Ventura rivers at 10–15% of scenes (Fig. 6). After small and medium rainstorms (0.25–2.5 cm) plumes near the river mouths were observed at >50% of scenes. Plumes propagated in both directions along the coast; the occurrence of plumes gradually decreased with the distance from river mouth. When the rainstorm exceeded 2.5 cm, the plume zone was observed along the entire coast and was much wider offshore. The plume pattern was symmetrical; no preference in plume propagation (poleward vs. equatorward) was detected.

In Santa Monica Bay after rainstorms <2.5 cm, plumes bounded by nLw555>1.3 mW cm^{-2} μm^{-1} sr^{-1} were so small that could not be readily detected from satellite observations. However, after heavy rains (>2.5 cm), plumes bounded by nLw555>1.3 mW cm^{-2} μm^{-1} sr^{-1} did occur along the entire local coast, with the frequency of plume occurrence decreasing rapidly offshore (Fig. 7F). As such, the apparent influence of rainstorms on the optical properties of surface waters in Santa Monica Bay was seemingly not as great as in the other regions. The best correlation between precipitated stormwater and plume area was observed when the plume threshold was smaller (nLw555>0.8 mW cm^{-2} μm^{-1} sr^{-1}) as compared with Ventura, San Pedro Shelf, and Orange County/San Diego (nLw555>1.3 mW cm^{-2} μm^{-1} sr^{-1}). Within Santa Monica Bay, when the plumes were bounded by nLw555=0.8 mW cm^{-2} μm^{-1} sr^{-1}, even during dry periods (accumulated precipitation <0.25 cm) small plumes were observed inshore at 5–10% of scenes (Fig. 7A). After rainstorms 0.25–2.5 cm, plumes occurred more frequently, with a maximum occurrence near the mouth of Ballona Creek (Fig. 7B–D). After strong rainstorms (>2.5 cm), the entire area of Santa Monica Bay was covered by plumes; near the mouth of Ballona Creek plumes were observed in >50% of scenes (Fig. 7E).

In the San Pedro Shelf region dry season (rain <0.25 cm) plumes were observed at 10–15% of the time at the mouth of the Los Angeles and San Gabriel rivers (Fig. 8). The width of

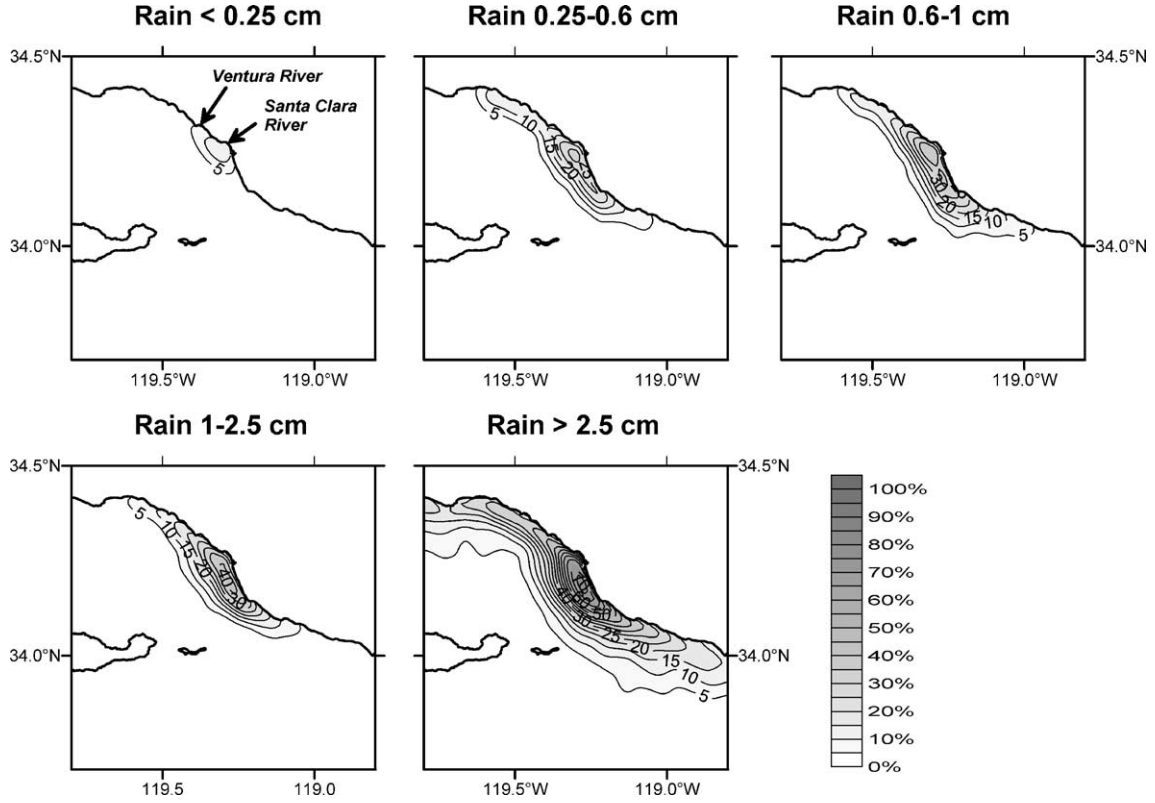

Fig. 6. The areas occupied by freshwater plume after rainstorms of different magnitude in Ventura region. The isolines indicate the percentage of satellite images with nLw555>1.3 mW cm^{-2} μm^{-1} sr^{-1}; the resulting grids were smoothed by 5-km cosine-filter.

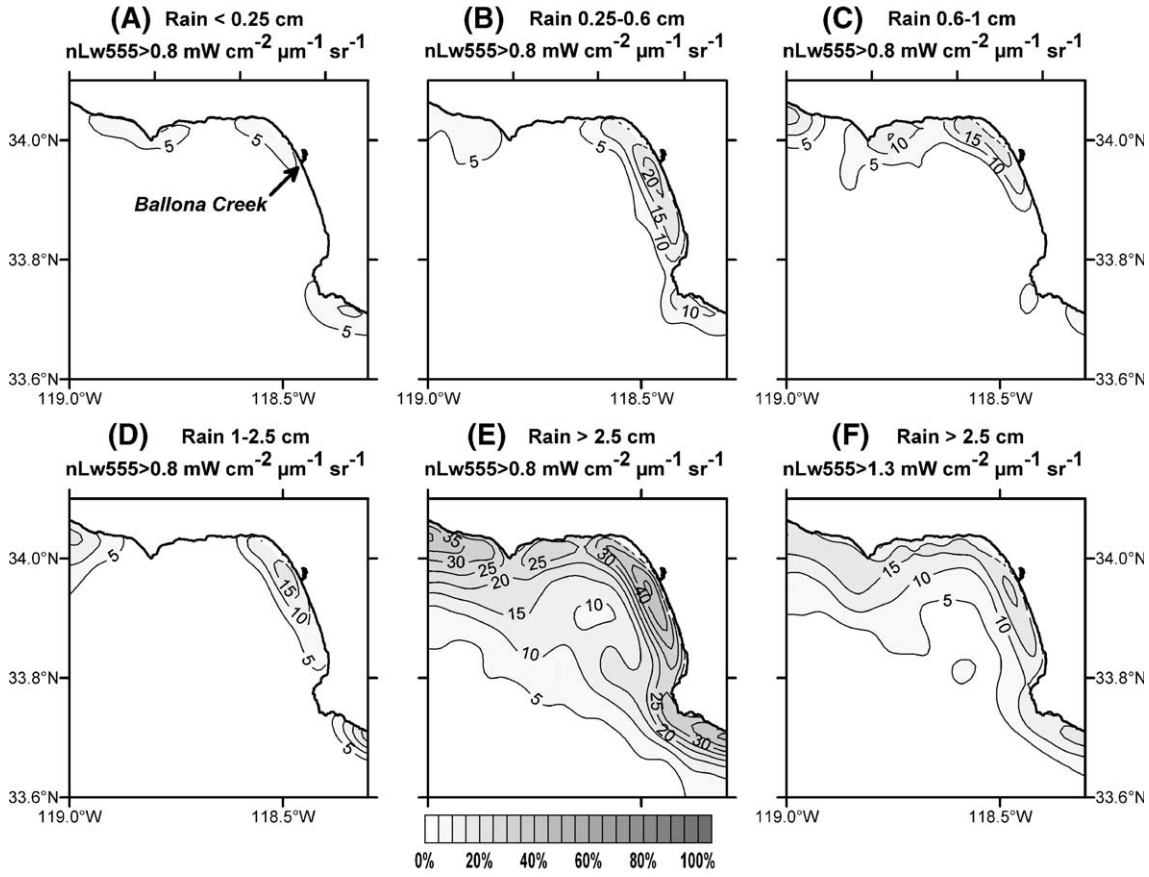

Fig. 7. The areas occupied by freshwater plume after rainstorms of different magnitude in Santa Monica Bay. The isolines indicate the percentage of satellite images with nLw555>0.8 mW cm^{-2} μm^{-1} sr^{-1} (A–E) and nLw555>1.3 mW cm^{-2} μm^{-1} sr^{-1} (F); the resulting grids were smoothed by 5-km cosine-filter. No plumes with nLw555>1.3 mW cm^{-2} μm^{-1} sr^{-1} were detected after rainstorms <2.5 cm.

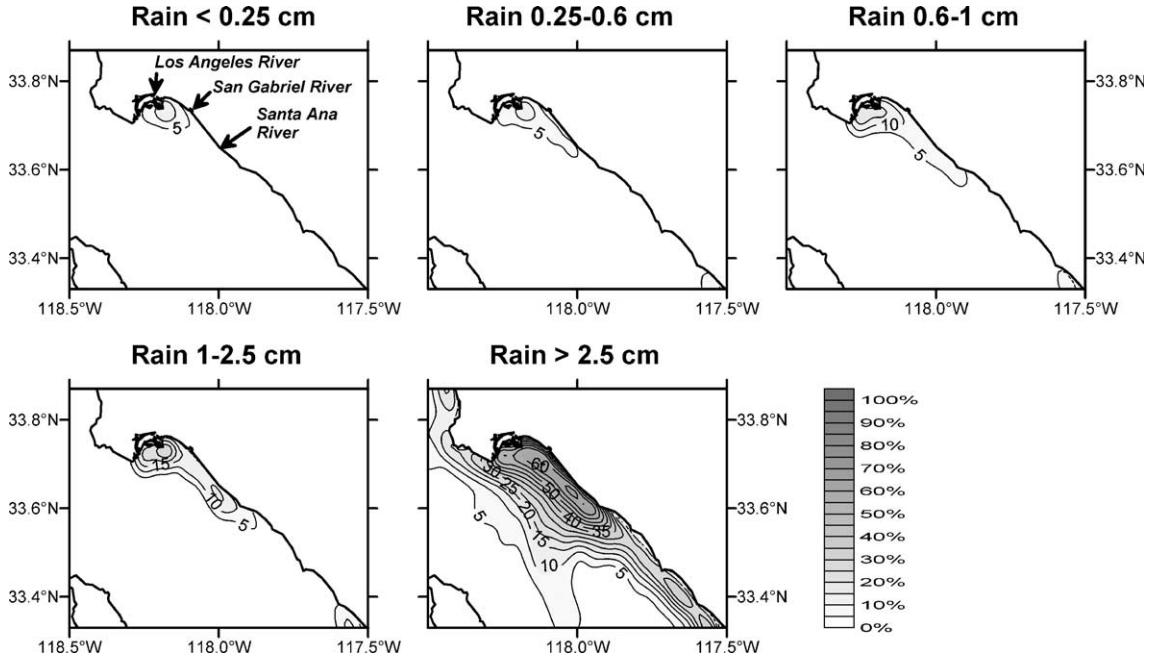

Fig. 8. The areas occupied by freshwater plume after rainstorms of different magnitude over San Pedro Shelf. The isolines indicate the percentage of satellite images with nLw555>1.3 mW cm^{-2} μm^{-1} sr^{-1}; the resulting grids were smoothed by 5-km cosine-filter.

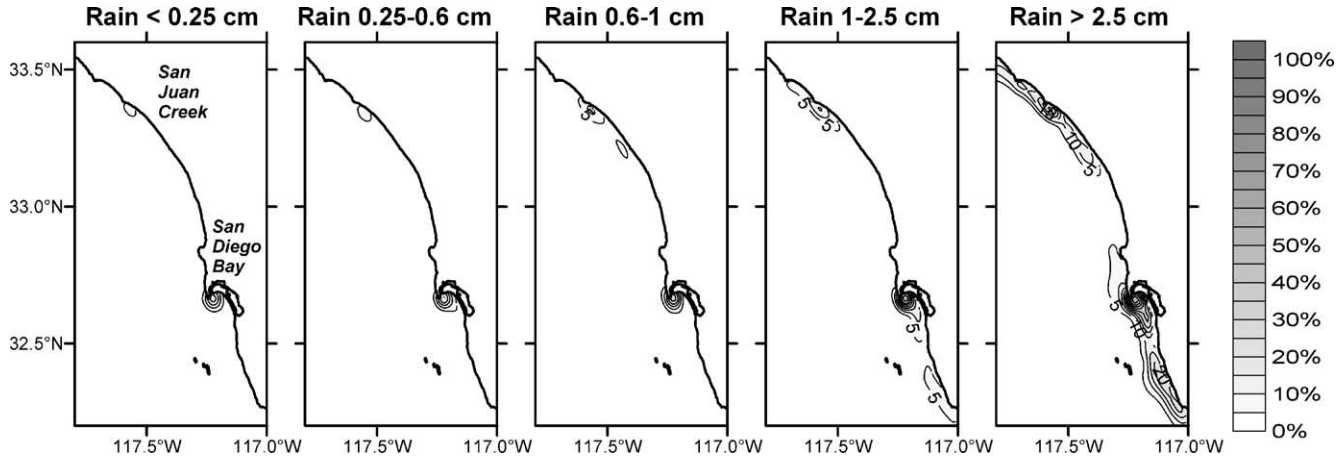

Fig. 9. The areas occupied by freshwater plume after rainstorms of different magnitude in Orange County/San Diego region. The isolines indicate the percentage of satellite images with nLw555>1.2 mW cm^{-2} μm^{-1} sr^{-1}; the resulting grids were smoothed by 5-km cosine-filter.

the zone where plumes were observed and the frequency of plumes increased with increasing rainstorm magnitude. After rains >2.5 cm, plumes were observed at almost all occasions along the coast from the mouth of Los Angeles River to the mouth of Santa Ana River. Plumes often propagated offshore in the south–southeastern direction.

In Orange County/San Diego region, plumes frequently (20–25% of scenes) occurred in the small zone near the mouth of San Diego Bay (Fig. 9) during both dry season and after rainstorms <1.0 cm. After rainstorms 1.0–2.5 cm, the frequency of plumes in this zone increased by 40–50%; small plumes were also observed along the San Juan Creek watershed. After strong rainstorms (>2.5 cm), plumes were observed at almost all occasions near San Diego Bay and at 10–20% of the time near the mouth of the San Juan Creek watershed, and to the south of San Diego Bay.

The elevation characteristics of all four watersheds were different (Fig. 10). In the watersheds adjacent to Santa Monica Bay, the terrain was substantially lower as compared with Ventura, San Pedro Shelf, and Orange County/San Diego regions. In the Santa Monica Bay watershed, >30% of the terrain was <100 m high (Fig. 10B); the elevation of most of the remaining area did not exceed 500 m. In the watershed adjacent to San Pedro Shelf about 15% of the terrain was <50 m (Fig. 10C). At the same time, 40% of the area of the watersheds adjacent to San Pedro Shelf exceeded 500 m. However, it is important to keep in mind that the total area of the watersheds draining to the San Pedro Shelf (i.e. Los Angeles, San Gabriel, and Santa Ana rivers) is almost an order of magnitude greater than the watershed area draining to Santa Monica Bay (Table 1). The elevation in the northern region (Ventura, Fig. 10A) was higher than in the other two regions; almost 30% exceeded 1000 m (cf., 21% in San Pedro, 15% in Orange County/San Diego, and 0% in Santa Monica Bay).

Land-use characteristics differed between the regions. Watersheds draining to the San Pedro Shelf and (to a lesser extent) to Santa Monica Bay are densely populated and urbanized. In contrast, watersheds draining the Ventura and Orange County/San Diego regions are less populated and contain more undisturbed area. About 40% of the watersheds adjacent to Santa Monica Bay and San Pedro Shelf were covered by impervious surfaces (Fig. 11B, C). In contrast, the impervious cover in the Ventura (Fig. 11A) and Orange County/San Diego (Fig. 11D) regions was much lower (7–14%). The total area of "pervious" lands where water

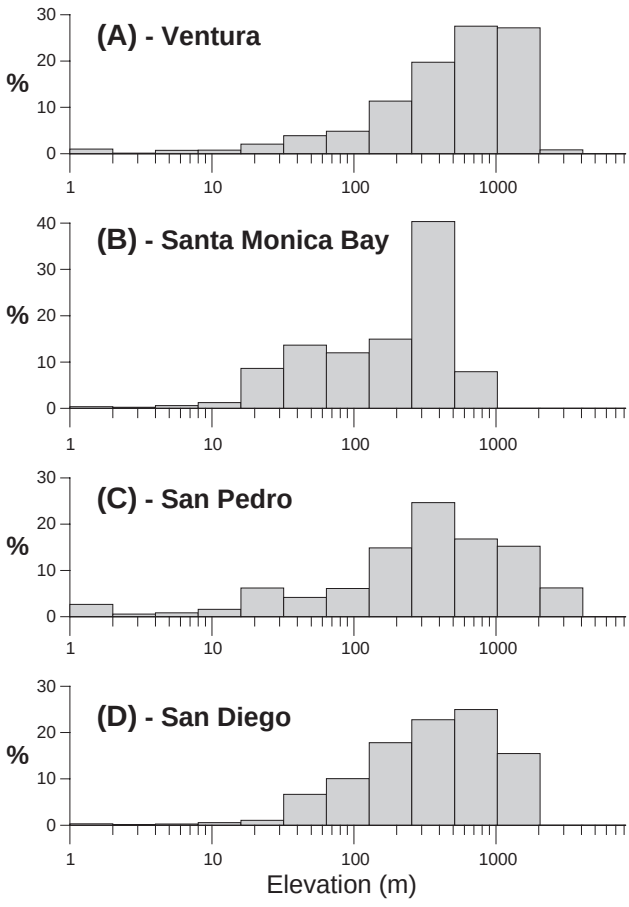

Fig. 10. Elevation of the watersheds of Ventura (A); Santa Monica Bay (B); San Pedro Shelf (C); Orange County/San Diego regions (D).

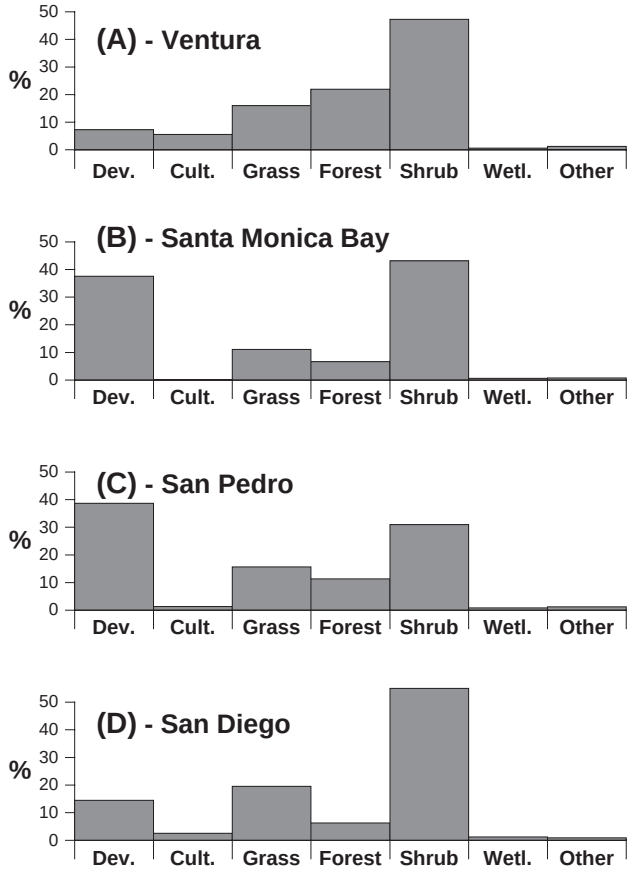

Fig. 11. Percentage of different land-use areas in the watersheds of Ventura (A); Santa Monica Bay (B); San Pedro Shelf (C); Orange County/San Diego region (D). Dev—developed land; Cult.—cultivated land; Grass—grasslands; Forest—deciduous, evergreen and mixed forests; Shrub—scrub/shrub areas; Wetl.—wetlands.

infiltrates (grasslands, forests, and shrubs) was 58–61% in Santa Monica Bay and San Pedro watersheds and 81–85% in Ventura and Orange County/San Diego regions.

5. Discussion

5.1. Backscattering index as a plume indicator

High correlation between accumulated stormwater and the areas of river plumes estimated on the basis of backscattering index (i.e., normalized water-leaving radiance of 555-nm wavelength nLw555; green–yellow band) indicates that the latter optical property is a good proxy of the amount of freshwater discharged to coastal ocean. This conclusion agrees with the results of previous studies. Otero and Siegel (2004) studying freshwater plumes in the northern part of the Southern California Bight showed that the SeaWiFS 555-nm band is better correlated with the concentration of suspended sediments than other bands. Toole and Siegel (2001) have shown that nLw555 was highly correlated with lithogenic silica concentration, which, in turn, is an important constituent of river discharge and was found to be a good indicator of suspended sediment concentration (Shipe et al., 2002; Warrick et al., 2004b).

The level of nLw555, which exceeded 1.3 mW cm^{-2} μm^{-1} sr^{-1}, was found to be a good indicator of river plumes in all study regions excluding Santa Monica Bay. A similar value was noted earlier by Otero (2002) for Santa Barbara Channel in the northern part of the Southern California Bight and by Nezlin and DiGiacomo (2005) over San Pedro Shelf. We can hypothesize, however, that high nLw555 can result not only from the runoff-discharged high sediment concentration, but also from high chlorophyll concentration related to elevated phytoplankton biomass (Kirk, 1994).

Otero (2002) and Toole and Siegel (2001) analyzed the nLw555 values in the mouth of the Santa Clara River in 1997–2001 and showed that under high chlorophyll concentration (>2 mg m^{-3}) nLw555 also increased but never exceeded 1.0–1.3 mW cm^{-2} μm^{-1} sr^{-1}. At the same time, within the Santa Clara River plume, nLw555 was much higher (4.6–11.1 mW cm^{-2} μm^{-1} sr^{-1}). A close agreement between the results of earlier studies and our observations provides a basis for recommendation to use the ocean surface optical property nLw555 = 1.3 mW cm^{-2} μm^{-1} sr^{-1} as an indicator of the boundary of freshwater plumes off southern California.

In this study, we focused on the correlation between stormwater and plume areas using indicator nLw555 values as a representative proxy, avoiding quantitative estimations of the concentration of suspended sediments. However, recent methodological studies provide an opportunity for evaluation of the amount of suspended sediments from satellite data (Acker et al., 2004; Miller & McKee, 2004; Warrick et al., 2004a). A comparison between these estimations and the results of the modeling of sediment and pollution discharge to the Southern California Bight (Ackerman & Schiff, 2003; Ackerman et al., 2005) will be a focus of our future work.

5.2. Quantitative relationship between the amount of stormwater and the plume area

The “accumulated stormwater” index estimated from daily rainfall (see Eq. (1)) is a better predictor of plume area than daily rainstorm magnitude. Consequently, it should be more useful to managers in making decisions regarding beach postings or closures. In all four regions we studied, the coefficients of determination (R^2) of rain/plume linear correlation appeared to be substantially higher after the time-series of precipitated water was transformed to “accumulated stormwater” using Eq. (1). Rainstorms in southern California are short episodic events. At the same time, the resulting plumes emerge during 1–2 days after the rainstorms and persist for several days, if not weeks. Transforming rainstorm time-series with Eq. (1) dramatically decreases its temporal variability, making its autocorrelation function similar to the autocorrelation function of plume dynamics (Nezlin & DiGiacomo, 2005). Estimating the “accumulated stormwater” index from daily precipitation, we take into account all antecedent rainstorms, weighting their contribution according to the time period between the rainstorm and the plume.

Zero intercept in linear regression equations between the accumulated stormwater and the size of plume area indicates

that rainfall was a primary source of the plumes observed in the SeaWiFS data set. The assumption that a substantial portion of stormwater was infiltrated and accumulated in the soil and in reservoirs would have resulted in negative intercept of linear regression (i.e., precipitation lower than some threshold was retained in the watersheds; only the stormwater exceeding this threshold flowed to the coastal ocean and produced plumes). An alternative hypothesis that the satellite-observed plumes were produced by factors other than stormwater (e.g., year-round domestic wastewater discharge, wind-driven sediment resuspension, phytoplankton blooms, etc.) would have resulted in positive intercept (i.e., plumes existed even in the absence of rainstorms). However, in all four regions the intercepts of linear equations were insignificantly different from zero, indicating rainfall as a most likely source of plumes along the southern California coast. We should keep in mind, however, that zero intercepts of the linear equations can partly result from the scatter in the data, particularly at the low end of the scale (i.e. small rain events); the coefficients of determination (R^2) of linear equations being within the range 0.42–0.72 (Table 1). In particular, plumes with nLw555>1.3 mW cm^{-2} μm^{-1} sr^{-1} (or >0.8 mW cm^{-2} μm^{-1} sr^{-1} in Santa Monica Bay) were often observed at zero precipitation, including dry periods (see Fig. 4) and can be explained by release of water from reservoirs and sediment resuspension. Also, zero plume areas were often observed after significant precipitation, which can be explained by water retention in reservoirs. These positive and negative residuals counterbalanced each other, resulting in zero intercepts.

Wind-driven sediment resuspension was not likely to be a source of increased nLw555 values in the Southern California Bight. Washburn et al. (1992) studied this process in the western part of San Pedro Shelf and observed high concentrations of sediments resuspended by water circulation only within 15 m of the bottom. In all the study regions here the ocean bottom exceeded 15 m within 1 km offshore; as such, the sediments resuspended from the bottom by winds, waves, and currents were not likely to be a significant factor for purposes of these analyses.

Continuous freshwater discharge from municipal waste sources cannot produce prominent nearshore plumes along the coast of southern California (Svejkovsky & Jones, 2001). Eganhouse and Venkatesan (1993) and Steinberger and Stein (2004) estimated the amount of this discharge as $1.4–1.6 \times 10^9$ m^3 $year^{-1}$, which is equal on the average to $3.8–4.4 \times 10^6$ m^3 day^{-1}. At the same time, even a minor rainstorm of 0.25 cm produces about 36×10^6 m^3 of freshwater discharge to the SCB. This value is a product of precipitation times the total area of the coastal watersheds, after removal of the watershed area upstream of dams, which is 14652 km^2 (Ackerman & Schiff, 2003). A moderate rainstorm of 1 cm produces a discharge that exceeds the municipal wastewater discharge by more than one order of magnitude. Freshwater runoff from storm events is primarily discharged to the coastal ocean during the first 1–2 days post-event, transporting significant loadings of suspended sediments whose concentration is especially high during the first few hours of the flux (Bertrand-Krajewski et al., 1998; Cristina & Sansalone, 2003). As such, the mass of sediments transported to the ocean during rainstorms is several orders of magnitude higher than during dry periods (Mertes & Warrick, 2001), and these sediments manifest themselves in large plumes that can be observed remotely from satellite platforms based on their optical signatures as described here.

In southern California, it is clear that a substantial portion of stormwater runs off the coastal land mass and is discharged to the adjoining ocean, contributing to plume formation. In a previous study in the San Pedro Shelf region, Nezlin and DiGiacomo (2005) estimated that the total amount of precipitated stormwater was close to the total amount of discharged freshwater producing the plume, based on the coefficients of a linear "rain/plume" equation, the size of watershed area, and published measures of plume salinity. In this study, we showed that the relationship between stormwater and plume size could be described by a linear equation with zero intercept not only on the San Pedro Shelf, but also in other regions of southern California as well. Hence, the speculations of Nezlin and DiGiacomo (2005) are likely applicable to all coastal regions of southern California. The slopes of the linear equations from this study vary within the range of 52–130 (Table 3), which differs from the slope coefficient of the equation estimated for San Pedro Shelf (94.2) by ±50%. As such, the size of the plume area in the Ventura region was more than twice the plume size produced by a similar-sized rainstorm event in the Orange County/San Diego region. As described in the following section, this difference leads to a consideration of watershed features as a principal factor influencing the relationship and correlation between stormwater and plume dynamics.

5.3. Watershed characteristics influencing the "rain/plume" relationship

The land-use properties of the drainage area where the discharge is formed appeared to be a primary factor regulating the quantitative relationship between stormwater and plume dynamics. The size of watershed area and its terrain also influenced this relationship. We realize that proper comparison between the watersheds in terms of their hydrology should be done using hydrological models of freshwater discharge, which take into account the detailed description of watershed physiography and land use. The amount of discharged water and pollutants from different areas of southern California has been modeled using the Hydrologic Simulation Program-Fortran (HSPF) (Ackerman & Schiff, 2003; Ackerman et al., 2005). Modeling results illustrate that each km^2 of highly urbanized watershed contributes about twice the volume of total discharge than less urbanized areas (Ackerman & Schiff, 2003). In this current study, we used a less formal approach, based on a qualitative comparison between the watersheds vis-à-vis their quantitative characteristics: the size of watershed area (Table 1), watershed terrain (Fig. 10), and land-use properties (Fig. 11). Also, the systems of hydrologic control (dams and reservoirs) are also taken into account. As a result,

the general pattern observed (e.g., the differences between plume size, the slope coefficients in the linear rainfall/plume equations, etc.) is similar to the modeled results.

The size of the aggregated watershed area was not a primary factor regulating the typical size of the plumes observed in the nearshore coastal waters off southern California. This result can be attributed to the fact that each of the four areas analyzed consisted of multiple watersheds, each with its own characteristics; thereby diminishing the effect of each individual watershed on plume size. However, when the difference between the aggregated watershed areas was dramatic, the rain/plume relationships were qualitatively different; e.g., in the smallest watershed of Santa Monica Bay, the plume characteristics were different from the three other study regions. At the same time, when we compared the Ventura, San Pedro, and Orange County/San Diego regions, no direct correlation was revealed between the watershed area and the typical plume size. Largest plumes were observed in the Ventura region (see Table 3 and Fig. 5), whose watersheds were not the largest; both the San Pedro and Orange County/San Diego watersheds exceeded Ventura in terms of area size (8762–9320 km^2 vs. 6831 km^2). Previous studies (Mertes & Warrick, 2001; Warrick & Fong, 2004) of the quantitative relationship between the drainage (A) and river plume (P) areas indicated that these two parameters exhibited a power relationship ($P=c*A^b$). We explain this apparent contradiction by the fact that in this study we aggregated discharge estimates from multiple watersheds of different size, land use, hydrologic control, intrinsic sediment yield, etc., rather than individual watersheds with similar elevation and land-use characteristics. This aggregation likely confounded our ability to discern a clear relationship between watershed area and plume size.

According to our results, only in Santa Monica Bay did a smaller watershed area (1170 km^2) result in much smaller plumes. In this region, only heavy rains (>2.5 cm) produced optical plume signatures comparable with the other three regions. Small and moderate rainstorms (<2.5 cm) contributed to detectable plume signatures, but this influence was much weaker than in other regions, resulting in a lower nLw555 estimated as the optimal plume boundary indicator. As such, freshwater plumes in Santa Monica Bay were qualitatively different from the plumes observed in the Ventura, San Pedro, and Orange County/San Diego regions. We attribute this difference to a combination of size, terrain and land-use characteristics of the Santa Monica Bay catchment area, as well as watershed orientation and other intrinsic watershed properties. Specifically, Santa Monica Bay receives runoff from a broad range of land-use types (developed vs. natural) that drain directly to the ocean via short, steep watersheds. In contrast, other watersheds are less heterogeneous and/or have larger areas to integrate different runoff sources.

The land-use characteristics of the watershed area influenced the interval between the rainstorm and the resulting plume. In the San Pedro region, where almost 40% of the drainage area were classified as "developed", the period between a rainstorm and a plume maximum was one day, vs. two days for the three other regions. In southern California, "developed" (industrial, commercial, and residential) areas are characterized by highly impervious surfaces (i.e. 40–85% impervious cover) (Ackerman et al., 2005), which have been shown to result in a greater proportion of precipitation translating to runoff in a shorter amount of time (Dunne & Leopold, 1978). Similarly, the "runoff coefficient" (i.e., the runoff to rainfall volume ratio) in "developed" areas was estimated as 0.39–0.64 vs. 0.06–0.10 in "natural" (agricultural and open) areas (Ackerman & Schiff, 2003). The effect of watershed impervious cover on runoff is amplified in the watersheds draining to the San Pedro shelf because most of the major rivers are lined with concrete, which further increases the magnitude and rate at which runoff reaches the coast (Gumprecht, 1999). However, it is important to note that the upper portions of the Los Angeles and San Gabriel watersheds are controlled by a series of dams and basins which capture much of rainfall from the upper watershed and prevent it from reaching the coast, especially during smaller storms. These dams have the greatest effect on upper, more natural portions of the watersheds, with the lower, urbanized portions of the watersheds being subject to less hydrologic control. Therefore, the difference in effective land-use (i.e. the proportion of watershed land use not controlled by dams) between watersheds in the San Pedro region and other regions (Fig. 11) is even more dramatic. Based on effective land-use, impervious cover of the watersheds of Ventura and Orange County/San Diego regions is <10%. As a result, the relative amount of infiltrated water is higher and the time period of runoff flow to the ocean is longer. On the other hand, a slower flux of stormwater to the ocean resulted in more persistent plumes in Ventura and Orange County/San Diego areas, as compared with San Pedro Shelf (the "coefficients of persistence" are 0.89–0.90 vs. 0.75). These coefficients indicate that, according to the primitive model we used in this study, in the San Pedro Shelf region 75% of stormwater was retained in the plume and 25% dissipated daily. In contrast, in the Ventura and Orange County/San Diego regions 90% of stormwater was retained in the plumes and only 10% dissipated. One explanation of this difference is a slower freshwater discharge, resulting in a slower response in terms of the optical signature in the coastal waters. Another explanation is the difference in coastal circulation. We hypothesize that in the shallow near-shore zone of the San Pedro Shelf, small-scale and mesoscale variability of ocean circulation was more intensive than in deeper Ventura and Orange County/San Diego regions (e.g., DiGiacomo & Holt, 2001; Hickey, 1992), resulting in quicker plume erosion. The specific impact of these oceanographic features will be a focus of our future studies.

One interesting result was that the apparent nature of satellite-detected plumes in Santa Monica Bay was qualitatively different than in the other regions, as the optimal nLw555 backscattering coefficient serving as a local plume-indicator was substantially lower (0.8 vs. 1.3 mW cm^{-2} μm^{-1} sr^{-1}). Further, the time lag between rainstorms and plumes in the highly urbanized Santa Monica Bay watershed was two days, similar to the less developed Ventura and Orange County/San

Diego watersheds, but different, however, from the similarly urbanized San Pedro region, a seemingly anomalous result. In particular, comparing Santa Monica Bay to the San Pedro region, given their similarities in land-use characteristics (~40–85% development of watersheds) we assumed that the stormwater precipitated over this small watershed should flow to the ocean immediately after the rainstorm as is the case in the San Pedro region (Ackerman & Weisberg, 2003). However, the amount of stormwater accumulated over the Santa Monica Bay catchment area was relatively small overall, apparently impacting both the nature of the runoff (i.e., lower plume indicator value) as well as its timing, as discussed above. Another factor that distinguishes Santa Monica Bay from three other regions is its low elevation (Fig. 10B) decreasing the speed of water runoff. The correlation between accumulated stormwater and plume area in Santa Monica Bay was not lower than in other regions, however, indicating rainstorms were still primarily responsible for the observed variability in the plume characteristics.

The terrain of each watershed also contributed to the relationship between rainfall and nearshore plumes. Ventura and Orange County/San Diego regions are similar in terms of watershed size and land-use characteristics. At the same time, in the Ventura watershed, 28% of drainage area is elevated >1000 m above sea level, vs. 15% in the Orange County/San Diego watershed. As a result, the plumes characteristic of the Ventura region were substantially larger than the plumes observed in Orange County/San Diego region. Another contributing factor is that in the Ventura region the bulk of freshwater discharge is concentrated from the Santa Clara River, in contrast to the Orange County/San Diego region, where stormwater is discharged to the ocean through several small rivers and creeks. Among other factors causing smaller plumes off San Diego/Orange County are the effect of numerous dams and bimodal watershed physiography, especially in San Diego County, where river flow is often retained in the inland alluvial valleys. Also, the coastal plains in San Diego/Orange County have deep alluvial aquifers (that are not completely paved) allowing more infiltration. Coastal wetlands (Newport Bay, Bolsa Chica, Batiquitos, San Dieguito, San Elijo, etc.) also may attenuate runoff and reduce plumes. The estimations of sediment transport in different parts of the California coast (Mertes & Warrick, 2001) revealed that small rivers contribute more sediment to the ocean near-shore zone than large rivers. However, the comparison here between the Ventura and Orange County/San Diego watersheds does not support this concept, indicating other factors (e.g., the terrain) can also influence the relationship between rainstorm magnitude and plume area size. Our results partly corroborate the conclusion of Milliman and Syvitski (1992) that maximum elevation of the river basin is a primary factor regulating sediment loads.

More extensive sediment plumes from the outlets of the Santa Clara and Ventura rivers likely result from higher concentration of sediments in its discharge, because these rivers drain the highly erosive western Transverse Range of California and are understood to be the largest sediment source of the Southern California Bight (Schwalbach & Gorsline, 1985; Warrick et al., 2004b). Also, the mainstreams of these rivers do not have any major dams to capture sediment. In contrast, most other southern California watersheds have lower sediment yield and have major dams that control sediment flow to the coast (e.g., Santa Ana River, San Gabriel River, San Diego River). Different sediment production probably affects the satellite signatures of the plumes.

Satellite signatures of plumes may be affected not only by the concentration of sediments, but also by sediment deposition in the nearshore zone, which acts to dilute the plume. Sediment deposition is mainly a function of the particle-size distribution within the plume and local and remote wind and tidal forcing. Ahn et al. (2005) studied particle size spectra in the Santa Ana River plume and showed that it progressively coarsened during the first few days after the rainstorm. They explain this observation as a result of within-plume coagulation of particles into larger size classes and, ultimately, removal of the largest particles by gravitational sedimentation. However, we have no data on the differences between the sediment size structures in different SCB regions; hence, this hypothesis needs future investigation. Furthermore, local hydrodynamic conditions can influence the rate of plume dilution. These issues will also be a focus of our future studies.

Different shapes of power regression equations (Fig. 4; Table 3) also indicate the differences in land-use watershed characteristics as a primary factor influencing surface runoff. According to theoretical concepts developed by the Soil Conservation Service (see Carlson, 2004; Chow et al., 1988) the curve $P_e=(P-0.2\cdot S)^2/(P+0.8\cdot S)$ describing the relationship between the rainfall P and the excess (i.e., not infiltrated) precipitation P_e, which in turn forms the runoff, is linear when the land-use parameter S (called "potential maximum retention") is zero. S is very small in highly developed impervious areas and increases in natural landscapes where the infiltration rate is higher. At higher S the form of rainfall/runoff relationship becomes more curvilinear, which agrees well with the results of our observations. The rainfall/plume (i.e., the rainfall/runoff) equation in the San Pedro region was almost linear, resulting from its physiography and land-use favoring an unimpeded discharge of rainfall to the ocean. In other regions high infiltration rate in natural watersheds (Ventura and Orange County/San Diego) or low elevation (Santa Monica Bay) as well as watershed physiography increased water retention, resulting in slower discharge of polluted surface water to coastal ocean.

6. Summary and conclusions

In this study, we analyzed 1.1-km spatial resolution visible spectral radiance data acquired in 1997–2003 by the Sea-viewing Wide Field-of-view Sensor (SeaWiFS), focusing on four regions with distinctive adjacent watershed properties: Ventura, Santa Monica Bay, San Pedro Shelf, and Orange County/San Diego. The area of each plume was detected by the backscattering characteristics of surface waters, i.e., normalized water-leaving radiation of green–yellow wavelength 555 nm

(nLw555). This index was shown to be a good proxy of the amount of freshwater discharged to coastal ocean.

A primary factor regulating the plume size was the rainstorm magnitude, which was estimated from atmospheric precipitation averaged over the total area of the watersheds connected to the seashore. "Accumulated stormwater" index estimated from daily rainfall (see Eq. (1)) predicted the plume area at much higher confidence level than daily rainstorm magnitude.

Quantitative relationships between precipitation and plume characteristics were different in different regions. Plumes in Ventura region were substantially larger after similar rainstorms, as compared with three other regions. The primary factors regulating the relationship between rainstorm and plume were watershed land-use characteristics, size, and elevation. Most dramatic difference was revealed between San Pedro Shelf and other three regions. In particular, the time lag between rainstorm and maximum plume was one day in San Pedro Shelf and two days elsewhere. Another quantitative characteristic derived from maximum correlation between stormwater and plume size was the "coefficient of persistence", related to the speed of freshwater discharge and the time of plume water dissipation; it also indicated higher speeds of discharge and plume erosion in San Pedro Shelf than in other three regions. Impervious surfaces dominating in highly urbanized watersheds adjacent to San Pedro Shelf resulted in quick and linear "rain/plume" relationship; in other three regions this relationship was more curvilinear, indicating higher infiltration rate typical to natural landscapes.

Results from this work provide an improved understanding of stormwater runoff and plume distribution in the southern California coastal region, particularly in the context of accumulated rainfall and variable watershed characteristics. By developing robust satellite-derived indicators that can be used for local plume discrimination, as well as associated maps indicating historical plume coverage in local regions based on the amount of rainfall, we hope to facilitate transition of this work from a research and development activity into an operational capability that can be utilized by local coastal water quality managers and decision-makers. In this context, we believe this work also provides insights into other developing and developed urban coastal regions particularly vis-à-vis changes in land use associated with increasing urbanization.

Acknowledgements

The authors would like to thank the SeaWiFS Project (Code 970.2) and the Distributed Active Archive Center (Code 902) at the NASA Goddard Space Flight Center for the production and distribution of the SeaWiFS data and images, respectively. These activities are sponsored by NASA's Mission to Planet Earth Program. We also thank the NOAA National Data Center Climate Data Online (NNDC/CDO) for the rain gauge-measured precipitation data. Critical remarks by two anonymous reviewers helped to improve this paper substantially. The JPL effort was supported by the National Aeronautics and Space Administration through a contract with the Jet Propulsion Laboratory, California Institute of Technology.

References

Acker, J. G., Shen, S., Leptoukh, G., Serafino, G., Feldman, G., & McClain, C. (2002). SeaWiFS ocean color data archive and distribution system: Assessment of system performance. *IEEE Transactions on Geoscience and Remote Sensing*, *40*, 90–103.

Acker, J. G., Vasilkov, A. P., Nadeau, D., & Kuring, N. (2004). Use of SeaWiFS ocean color data to estimate neritic sediment mass transport from carbonate platforms for two hurricane-forced events. *Coral Reefs*, *23*, 39–47.

Ackerman, D., & Schiff, K. (2003). Modeling storm water mass emissions to the Southern California Bight. *Journal of Environmental Engineering*, *129*, 308–317.

Ackerman, D., Schiff, K. C., & Weisberg, S. B. (2005). Evaluating HSPF in an arid, urbanized watershed. *Journal of American Water Resources Association*, *41*, 477–486.

Ackerman, D., & Weisberg, S. B. (2003). Relationship between rainfall and beach bacterial concentrations on Santa Monica Bay beaches. *Journal of Water and Health*, *1*, 85–89.

Ahn, J. H., Grant, S. B., Surbeck, C. Q., DiGiacomo, P. M., Nezlin, N. P., & Jiang, S. (2005). Coastal water quality impact of stormwater runoff from an urban watershed in southern California. *Environmental Science and Technology*, *39*, 5940–5953.

Bailey, H. P. (1966). *The climate of southern California*. Berkley: University of California Press. 87 pp.

Bay, S., Jones, B. H., Schiff, K., & Washburn, L. (2003). Water quality impacts of stormwater discharges to Santa Monica Bay. *Marine Environmental Research*, *56*, 205–223.

Bertrand-Krajewski, J. -L., Chebbo, G., & Saget, A. (1998). Distribution of pollutant mass vs volume in stormwater discharges and the first flush phenomenon. *Water Research*, *32*, 2341–2356.

Beuhler, M. (2003). Potential impacts of global warming on water resources in southern California. *Water Science and Technology*, *47*, 165–168.

Booth, D. B. (1990). Stream channel incision following drainage basin urbanization. *Water Resources Bulletin*, *26*, 407–417.

Cabelli, V. J., Dufour, A. P., McCabe, L. J., & Levin, M. A. (1982). Swimming-associated gastroenteritis and water quality. *American Journal of Epidemiology*, *115*, 606–616.

Carlson, T. N. (2004). Analysis and prediction of surface runoff in an urbanizing watershed using satellite imagery. *Journal of the American Water Resources Association*, *40*, 1087–1098.

Chow, V. T., Maidment, D. R., & Mays, L. W. (1988). *Applied hydrology*. New York, New York: McGrow-Hill Book Company. 572 pp.

Cristina, C. M., & Sansalone, J. J. (2003). "First flush", power law and particle separation diagrams for urban storm-water suspended particulates. *Journal of Environmental Engineering*, *129*, 298–307.

DiGiacomo, P. M., & Holt, B. (2001). Satellite observations of small coastal ocean eddies in the Southern California Bight. *Journal of Geophysical Research*, *106*, 22521–22543.

Dorman, C. E., & Winant, C. D. (1995). Buoy observations of the atmosphere along the West Coast of the United States. *Journal of Geophysical Research*, *100*, 16029–16044.

Dunne, T., & Leopold, L. B. (1978). *Water in environmental planning*. San Francisco: W.H.Freeman Publishers. 818 pp.

Eganhouse, R. P., & Venkatesan, M. I. (1993). Chemical oceanography and geochemistry. In M. D. Dailey, D. J. Reish, & J. W. Anderson (Eds.), *Ecology of the Southern California Bight* (pp. 71–189). Berkeley: University of California Press.

Esaias, W. E., Abbott, M. R., Barton, I., Brown, O. B., Campbell, J. W., & Carder, K. L., et al. (1998). An overview of MODIS capabilities for ocean science observations. *IEEE Transactions on Geoscience and Remote Sensing*, *36*, 1250–1265.

Gumprecht, B. (1999). *The Los Angeles river. Its life, death, and possible rebirth*. Baltimore: The Johns Hopkins University Press. 372 pp.

Haile, R. J., Witte, J. S., Gold, M., Cressey, R., McGee, C., & Millikan, R. C., et al. (1999). The health effects of swimming in ocean water contaminated by storm drain runoff. *Epidemiology*, *10*, 355–363.

Hickey, B. M. (1992). Circulation over the Santa Monica–San Pedro basin and shelf. *Progress in Oceanography*, *30*, 37–115.

Kirk, J. T. O. (1994). *Light and photosynthesis in aquatic ecosystems*. Cambridge: Cambridge University Press. 509 pp.

Lu, R., Turco, R. P., Stolzenbach, K., Friedlander, S. K., Xiong, C., & Schiff, K., et al. (2003). Dry deposition of airborne trace metals on the Los Angeles Basin and adjacent coastal waters. *Journal of Geophysical Research*, *108*, 4074.

McClain, C. R., Feldman, G. C., & Hooker, S. B. (2004). An overview of the SeaWiFS project and strategies for producing a climate research quality global ocean bio-optical time series. *Deep-Sea Research II*, *51*, 5–42.

Mertes, L. A. K., Hickman, M., Waltenberger, B., Bortman, A. L., Inlander, E., & McKenzie, C., et al. (1998). Synoptic views of sediment plumes and coastal geography of the Santa Barbara Channel, California. *Hydrological Processes*, *12*, 967–979.

Mertes, L. A. K., & Warrick, J. A. (2001). Measuring flood output from 110 coastal watersheds in California with field measurements and SeaWiFS. *Geology*, *29*, 659–662.

Miller, R. L., & McKee, B. A. (2004). Using MODIS Terra 250 m imagery to map concentrations of total suspended matter in coastal waters. *Remote Sensing of Environment*, *93*, 259–266.

Milliman, J. D., & Syvitski, J. P. M. (1992). Geomorphic/tectonic control of sediment discharge to the ocean: The importance of small mountainous rivers. *Journal of Geology*, *100*, 525–544.

Nezlin, N. P., & DiGiacomo, P. M. (2005). Satellite ocean color observations of stormwater runoff plumes along the San Pedro Shelf (southern California) during 1997 to 2003. *Continental Shelf Research*, *25*, 1692–1711.

Nezlin, N. P., & Stein, E. D. (2005). Spatial and temporal patterns of remotely-sensed and field-measured rainfall in southern California. *Remote Sensing of Environment*, *96*, 228–245.

Noble, R. T., Weisberg, S. B., Leecaster, M. K., McGee, C. D., Dorsey, J. H., & Vainik, P., et al. (2003). Storm effects on regional beach water quality along the southern California shoreline. *Journal of Water and Health*, *1*, 23–31.

Otero, M.P., (2002). Spatial and temporal characteristics of sediment plumes and phytoplankton blooms in the Santa Barbara Channel. M.S. Thesis, University of California Santa Barbara. 113 pp.

Otero, M. P., & Siegel, D. A. (2004). Spatial and temporal characteristics of sediment plumes and phytoplankton blooms in the Santa Barbara Channel. *Deep-Sea Research II*, *51*, 1129–1149.

Reeves, R. L., Grant, S. B., Mrse, R. D., Copil Oancea, C. M., Sanders, B. F., & Boehm, A. B. (2004). Scaling and management of fecal indicator bacteria in runoff from a coastal urban watershed in southern California. *Environmental Science and Technology*, *38*, 2637–2648.

Sathyendranath, S. (Ed.) (2000). Remote sensing of ocean colour in coastal and other optically-complex waters. Vol. 3. Reports of the International Ocean-Colour Coordinating Group. IOCCG. 140 pp.

Schiff, K. C., Allen, M. J., Zeng, E. Y., & Bay, S. M. (2000a). Southern California. *Marine Pollution Bulletin*, *41*, 76–93.

Schiff, K. C., Allen, M. J., Zeng, E. Y., & Bay, S. M. (2000b). Southern California. In C. R. C. Sheppard (Ed.), *Seas at the millennium: An environmental evaluation* (pp. 385–404). Amsterdam: Pergamon.

Schiff, K. C., & Bay, S. (2003). Impacts of stormwater discharges on the nearshore benthic environment of Santa Monica Bay. *Marine Environmental Research*, *56*, 225–243.

Schwalbach, J. R., & Gorsline, D. S. (1985). Holocene sediment budgets for the basins of the California continental borderland. *Journal of Sedimentary Petrology*, *55*, 829–842.

Shipe, R. F., Passow, U., Brzezinski, M. A., Graham, W. M., Pak, D. K., & Siegel, D. A., et al. (2002). Effects of the 1997–98 El Nino on seasonal variations in suspended and sinking particles in the Santa Barbara basin. *Progress in Oceanography*, *54*, 105–127.

Steinberger, A., & Stein, E. D. (2004). Effluent discharges to the Southern California Bight from large municipal wastewater treatment facilities in 2001 and 2002. In S. B. Weisberg, & D. Elmore (Eds.), *Southern California coastal water research project. Annual Report 2003–2004* (pp. 2–15). Westminster, CA: Southern California Coastal Water Research Project Authority.

Svejkovsky, J., & Jones, B. (2001). Satellite imagery detects coastal stormwater and sewage runoff. *EOS*, *82*, 621–630.

Toole, D. A., & Siegel, D. A. (2001). Modes and mechanisms of ocean color variability in the Santa Barbara Channel. *Journal of Geophysical Research*, *106*, 26985–27000.

USGS (1996). GTOPO30. [Available online from http://edcdaac.usgs.gov/gtopo30/gtopo30.asp.].

Warrick, J. A., & Fong, D. A. (2004). Dispersal scaling from the world's rivers. *Geophysical Research Letters*, *31*, L04301.

Warrick, J. A., Mertes, L. A. K., Siegel, D. A., & MacKenzie, C. (2004a). Estimating suspended sediment concentrations in turbid coastal waters of the Santa Barbara Channel with SeaWiFS. *International Journal of Remote Sensing*, *25*, 1995–2002.

Warrick, J. A., Mertes, L. A. K., Washburn, L., & Siegel, D. A. (2004b). A conceptual model for river water and sediment dispersal in the Santa Barbara Channel, California. *Continental Shelf Research*, *24*, 2029–2043.

Washburn, L., Jones, B. H., Bratkovich, A. W., Dickey, T. D., & Chen, M. -S. (1992). Mixing, dispersion, and resuspension in vicinity of ocean wastewater plume. *Journal of Hydraulic Engineering*, *118*, 38–58.